# Enhanced binding of trigonal DNA-carbohydrate conjugates to lectin.

Matsui, Masayuki

Ebara, Yasuhito

(Citation)
Bioorganic & Medicinal Chemistry Letters,22(19):6139-6143

(Issue Date)
2012-10-01

(Resource Type)
journal article

(Version)
Accepted Manuscript

(URL)
https://hdl.handle.net/20.500.14094/90001823

# Enhanced Binding of Trigonal DNA-Carbohydrate Conjugates to Lectin

Masayuki Matsui[a,1], Yasuhito Ebara[b]

[a] Graduate School of Science and Technology, Kobe University, 3-11 Tsurukabuto, Nada-ku, Kobe 657-8501, Japan

[b] Graduate School of Human Development and Environment, Kobe University, 3-11 Tsurukabuto, Nada-ku, Kobe 657-8501, Japan

[1] Present Address: Department of Pharmacology, University of Texas Southwestern Medical Center at Dallas, 6001 Forest Park Road, Dallas, Texas 75390-9041, USA

Corresponding author: Yasuhito Ebara

E-mail: ebara@kobe-u.ac.jp

Phone: +81-78-803-7759

FAX +81-78-803-7761

**Keywords**: DNA-carbohydrate conjugate, glycocluster, multivalent interaction, lectin, 3-way junction DNA

**Abstract**—Novel trigonal DNA-carbohydrate conjugates were prepared and evaluated to explore efficient carbohydrate-lectin interactions. Carbohydrate-modified oligonucleotides were enzymatically prepared, then hybridized to form 3-way junction DNAs. The thermal stabilities of the junctions were assessed by UV melting analysis and formation of constructs was confirmed by gel electrophoresis. Fluorescence titration assays revealed that the trigonal DNA-carbohydrate conjugates exhibit high affinity to lectins depending on the distribution of carbohydrates presented in each arm. These results suggest that self-assembled 3-way DNA architectures could offer a useful platform for controlling the spatial distribution of carbohydrates on conjugates and achieving more efficient molecular recognition.

Carbohydrate-lectin interactions occur in a variety of biological events including inflammation, viral infection, cancer metastasis, and binding of bacterial toxins.[1–3] Although the interactions between monovalent carbohydrates and lectins are relatively weak ($10^3$–$10^4$ $M^{-1}$), affinity and specificity in such molecular recognition events are increased through multivalent interaction, which is known as the "glycoside cluster effect".[4] Over the past few decades, glycoconjugates have been developed using various matrixes such as polymers,[5] cyclodextrins,[6] peptides,[7,8] calixarenes,[9] dendrimers,[10] DNAs,[11–16] and carbon nanostructures.[17,18] They have been used to explore the mechanism of glycoside cluster effects,[4,19] develop inhibitors or biosensors for pathogenic lectins,[20–22] and achieve tissue-specific delivery of therapeutic oligonucleotides.[23]

Oligonucleotides have proven remarkably useful in many applications because of their ability to self-assemble in a predictable manner based on sequence complementarity.[24–26] They can also be highly functionalized with various chemical reporters and effectors.[27] Matsuura and co-workers have previously synthesized DNA-carbohydrate conjugates by using phosphoramidite chemistry,[12–14] diazo coupling methods,[11] or photocrosslinking[15] and reported their cooperative effects on lectin binding.[11–14] However, their glycoconjugates present a limited number of carbohydrates in the context of a DNA double helix or are not structurally homogeneous. Thus it is likely that their binding to lectins might be suboptimal. We hypothesized that it might be possible to use different DNA architectures to present carbohydrates with correct orientations and achieve more efficient multivalent interaction with lectins.

Here we describe novel trigonal DNA-carbohydrate conjugates designed for efficient multivalent interaction to lectins (Figure 1A). Using a branched DNA structure enables us to prepare structurally diverse glycoconjugates and facilitates controlling the spatial distribution of carbohydrates on the conjugates. Indeed, the distribution and orientation of carbohydrates on 3-way junction DNAs affects their affinity to lectins. DNA-carbohydrate conjugates thus show significant potential as multivalent glycoclusters.

We chose concanavalin A (Con A) as our initial target. Con A, which is isolated from *Canavalia ensiformis* (Jack bean) seeds, has been widely used and well characterized in its structure[28,29] and carbohydrate-binding specificity.[30,31] The lectin specifically binds to

α-D-glucose and α-D-mannose. Con A has a tetrameric form at neutral pH and each subunit has one binding site. The four binding sites are approximately 65 Å apart from one another (Figure 1B). As three of these binding sites are distributed in a triangle shape, Con A is an appropriate target for testing trigonal glycoconjugates. Such a triangular distribution of binding sites is also found in other lectins, including mannose binding protein (MBP-A)[32] and influenza hemagglutinin (HA).[33]

The oligonucleotide sequences used for constructing 3-way junction DNAs need to be carefully designed to form stable junctions with minimal unintended hybridization. After a computational screening based on sequence complementarity and thermal stabilities using nearest neighbor parameters, we selected one set of 18–20-mer sequences (Strand I, II, and III; Figure 2A) that are suitable to form 3-way junction DNAs.

The stability and conformation of 3-way junction complexes can be affected by such parameters as unpaired bases in the branch junction region.[34–36] We prepared Strand I, II, and III with different numbers of unpaired bases (0, 1, or 2; Figure 2A) and analyzed the mixtures I, I+II, and I+II+III by gel electrophoresis. As shown in Figure 2B, stepwise band patterns were observed, confirming that the three strands were correctly hybridized. We further characterized the formation of the complexes in the absence or presence of $Mg^{2+}$ by UV melting experiments. The melting profiles for each complex I+II+III appear to represent a typical two-state transition through the temperature range of 20–60°C, whether 0, 1, or 2 unpaired bases were included at the junctions (Figures 2C and 2D). The melting temperatures ($T_m$) for the complexes I+II+III increased as the number of unpaired bases at the junctions increased, suggesting that incorporation of unpaired bases releases strain in the junction region. Higher $Mg^{2+}$ concentrations also stabilized the complexes, as previously observed.[34,35] Thus the remainder of the study was carried out using sequences with two unpaired adenosines in the presence of $Mg^{2+}$. The 3' end of each strand was extended with carbohydrate-modified nucleotides (Figure 3B). We hypothesized that the flexibility of the unpaired junction region and the single stranded carbohydrate-modified region might facilitate the optimal binding of carbohydrate groups to lectin binding sites.

We previously reported an efficient method to construct carbohydrate-modified DNAs using DNA polymerase.[37] By using maltose- or lactose-modified dUTP as substrates for KOD

Dash DNA polymerase, we enzymatically incorporated maltose or lactose residues into 29–47-mer DNA oligonucleotides (Figures 3A and 3B, Table S1). Three of the synthesized carbohydrate-modified or unmodified oligonucleotides were mixed and annealed to prepare multiple trigonal DNAs with different modification patterns (Figures 3D and S1). Gel electrophoretic analysis of the constructs showed the stepwise change in band positions for the unmodified monomer, dimer, and trimer (Figure 3E, lanes 1–3). A similar stepwise band shift was observed for 3-way junction DNAs as the number of maltose residues incorporated into the complexes increased from the fully unmodified **S6(0,0,0)** through the partially modified **S6(M,0,0)** and **S6(M,M,0)** to the fully modified **S6(M,M,M)** (Figure 3E, lanes 3–6). These results demonstrate that carbohydrate-modified trigonal DNAs can be correctly formed by mixing and annealing the three complementary oligonucleotides. Fully double-stranded 59-bp unmodified and maltose-modified DNAs (**ds-Native** and **ds-Mal18**, respectively; Figures 3C and 3D) were also prepared through primer extension reactions and the products were confirmed by gel electrophoresis (Figure 3F).

Fluorescence titration assays were performed to evaluate the binding constants ($K_a$) of the complexes to Con A. We observed a significant decrease in fluorescence from FITC-labeled maltose-modified complexes with increasing concentrations of Con A solutions (Figure 4A). The $K_a$ of each complex for Con A was determined by analyzing the change in fluorescence intensity (F) at 521 nm as a function of Con A concentration (Table 1, Figure S3).

To investigate how the distribution of carbohydrates on 3-way junction DNAs affects their affinity to Con A, a series of 3-way junction DNAs, **S6(M,M,M)**, **S6(M,M,0)**, **S6(M,0,0)**, and **S6(0,0,0)** were assessed and compared (Figure 4B, Table 1). Of the four constructs, **S6(M,M,M)** bearing 6 maltose residues on each arm showed the highest affinity for Con A ($K_a = 1.0 \times 10^6\ M^{-1}$). This is about 12- and 83-fold higher than those of **S6(M,M,0)** ($K_a = 8.4 \times 10^4\ M^{-1}$) and **S6(M,0,0)** ($K_a = 1.2 \times 10^4\ M^{-1}$), respectively. The unmodified **S6(0,0,0)** showed relatively little change in fluorescence up to $4 \times 10^{-5}\ M^{-1}$ of Con A concentration, suggesting that it has no significant interaction with Con A. These results suggest that adequate localization of carbohydrates along the 3-way junction structure can lead to more efficient interaction for Con A which has a triangular distribution of the binding sites.

To test binding specificity, we performed competitive binding experiments using methyl-α-mannopyranoside (MeαMan), which is a monosaccharide specific for Con A. The affinity of **S6(M,M,M)** to Con A was greatly reduced when MeαMan was added at 50 mM as a competitor ($K_a$ = 5.1 × $10^4$ $M^{-1}$; Figure 4B), indicating that the interactions of **S6(M,M,M)** with Con A are mostly derived from specific carbohydrate-lectin interactions. Job's plot analysis was also performed to determine the binding stoichiometry. The analysis revealed a 1:1 binding of **S6(M,M,M)** to Con A (Figure S4).

The effect of the number of carbohydrates on the arms was moderate. **S12(M,M,M)** bearing 12 maltose residues in each arm showed a similar titration curve ($K_a$ = 7.9 × $10^5$ $M^{-1}$) relative to **S6(M,M,M)**, while **S3(M,M,M)** bearing 3 maltose residues in each arm showed 2.5-fold less affinity ($K_a$ = 4.0 × $10^5$ $M^{-1}$) than **S6(M,M,M)** (Figure 4C, Table 1). Thus all three trigonal 3-way junction DNAs **S3**, **S6**, and **S12(M,M,M)** maintain relatively high affinity. In contrast, reducing the number of modified arms had a strong negative effect on binding (e.g. **S6(M,0,0)** and **S6(M,M,0)**). Thus the spatial distribution of the carbohydrate residues is more important than the number of carbohydrates per arm.

We also focused on the effect of helical arrangement of carbohydrates on lectin recognition. **ds-S6(M,M,M)** has a 3-way junction structure but each arm is completely double-stranded, yielding a rigid structure that might be unable to optimize lectin binding interactions (Figures 3D and S2). **ds-Mal18** is a linear double-stranded DNA with 18 maltose residues (Figures 3C and 3D). Fluorescence titration assays revealed that both **ds-S6(M,M,M)** and **ds-Mal18** show much lower affinity to Con A compared with **S6(M,M,M)** which has single-stranded carbohydrate-modified regions (Figure 4C, Table 1), suggesting that the helical arrangement of carbohydrates along rigid double-stranded DNAs might restrict accessibility of carbohydrates to the multiple binding sites on Con A.

The affinity of **S6(M,M,M)** to Con A is more than 700-fold higher than that of monovalent maltose ($K_a$ = 1.31 × $10^3$ $M^{-1}$).[30] Furthermore, compared with the DNA-carbohydrate conjugates (mannosylated half-sliding oligonucleotides; $K_a$ = 2.4 × $10^4$ $M^{-1}$) reported by Yamada *et al.*,[14] the maltose-modified 3-way junction DNA showed much higher affinity for Con A. Thus 3-way junction structures can effectively distribute carbohydrate groups for high-affinity binding to Con A.

Finally we evaluated the affinity of lactose-modified 3-way junction DNAs to $RCA_{120}$ (*Ricinus Communis* Agglutinin I), which is a β-D-galactose-specific lectin. $RCA_{120}$ forms a tetramer and two active binding sites are located about 100Å away from each other (Figure S5).[38] We performed fluorescence titration assays to determine binding constants of lactose-modified 3-way junction DNAs to $RCA_{120}$ (Figure 4D, Table 1). The complexes **S6(L,L,L)** and **S6(L,L,0)** showed similar affinity to $RCA_{120}$ ($K_a = 0.63 \times 10^6\ M^{-1}$ and $1.0 \times 10^6\ M^{-1}$, respectively), while **S6(L,0,0)** and unmodified **S6(0,0,0)** didn't show any significant change in fluorescence, suggesting no significant interaction with the lectin. We speculate that carbohydrate modification in the two arms is probably sufficient for leading to efficient molecular recognition to $RCA_{120}$ which has only two active binding sites.

In conclusion, we successfully constructed maltose- or lactose-modified 3-way junction DNAs and observed the effect of self-organization of the carbohydrate-modified strands on lectin binding. These results indicate that self-assembled DNA architectures provide a useful platform for controlling the spatial distribution of carbohydrate groups, leading to more efficient glycoside cluster effects. By utilizing diverse DNA junctions and lattices, and changing the carbohydrate functionality appended to DNA, this approach might be applicable to other lectins with different binding-site topologies and make it possible to develop novel DNA-based nanodevices or inhibitors for various lectins.

**Acknowledgement**

This work was supported by Encouragement Research Assistance from Asahi Glass Foundation.

**References**

1. Mammen, M.; Choi, S.-K.; Whitesides, G. M. *Angew. Chem. Int. Ed.* **1998**, *37*, 2754–2794.
2. Lis, H.; Sharon, N. *Chem. Rev.* **1998**, *98*, 637–674.
3. Sacchettini, J. C.; Baum, L. G.; Brewer, C. F. *Biochemistry* **2001**, *40*, 3009–3015.
4. Lundquist, J. J.; Toone, E. J. *Chem. Rev.* **2002**, *102*, 555–578.
5. Bovin, N. V.; *Glycoconj. J.* **1998**, *15*, 431–446.
6. Fulton, D. A.; Stoddart, J. F. *Bioconjugate Chem.* **2001**, *12*, 655–672.

7. Ohta, T.; Miura, N.; Fujitani, N.; Nakajima, F.; Niikura, K.; Sadamoto, R.; Guo, C.-T.; Suzuki, T.; Suzuki, Y.; Monde, K.; Nishimura, S.-I. *Angew. Chem. Int. Ed.* **2003**, *42*, 5186–5189.
8. Sebestik, J.; Niederhafner, P., Jezek, J. *Amino Acids* **2011**, *40*, 301–370.
9. Dondoni, A.; Marra, A. *Chem. Rev.* **2010**, *110*, 4949–4977.
10. Turnbull, W. B.; Stoddart, J. F. *Rev. Mol. Biotechnol.* **2002**, *90*, 231-255.
11. Matsuura K.; Akasaka, T.; Hibino, M.; Kobayashi, K. *Bioconjugate Chem.* **2000**, *11*, 202–211.
12. Matsuura, K.; Hibino, M.; Yamada, Y.; Kobayashi, K. *J. Am. Chem. Soc.* **2001**, *123*, 357–358.
13. Matsuura, K.; Hibino, M.; Ikeda, T.; Yamada, Y.; Kobayashi, K. *Chem. Eur. J.* **2004**, *10*, 352–359.
14. Yamada, Y.; Matsuura, K.; Kobayashi, K. *Bioorg. Med. Chem.* **2005**, *13*, 1913–1922.
15. Kim, K.; Matsuura, K.; Kimizuka, N. Bioorg. Med. Chem. **2007**, *15*, 4311–4317.
16. Karskela, M.; Helkearo, M.; Virta, P.; Lönnberg, H. *Bioconjugate Chem.* **2010**, *21*, 748–755.
17. Chen, Y.; Vedala, H.; Kotchey, G. P.; Audfray, A.; Cecioni, S.; Imberty, A.; Vidal, S.; Star, A. *ACS Nano* **2012**, *1*, 760–770.
18. Cecioni, S.; Oerthel, V.; Iehl, J.; Holler, M.; Goyard, D.; Praly, J.-P.; Imberty, A.; Nierengarten, J.-F.; Vidal, S. *Chem. Eur. J.* **2011**, *17*, 3252–3261.
19. Deniaud, D.; Julienne, K.; Gouin, S. G. *Org. Biomol. Chem.* **2011**, *9*, 966–979.
20. Jelinek, R.; Kolusheva, S. *Chem. Rev.* **2004**, *104*, 5987–6015.
21. Sharon, N. *Biochim. Biophys. Acta* **2006**, *1760*, 527–537.
22. Zeng, X.; Andrade, C. A. S.; Oliveira, M. D. L.; Sun, X.-L. *Anal. Bioanal. Chem.* 2012, 402, 3161–3176.
23. Yan, H.; Tram, K. *Glycoconju. J.* **2007**, *24*, 107–123.
24. Seeman, N. C. *J. Theor. Biol.* **1982**, *99*, 237–247.
25. Feldkamp, U.; Niemeyer, C. M. *Angew. Chem. Int. Ed.* **2006**, *45*, 1856–1876.
26. Aldaye, F. A.; Palmer, A. L.; Sleiman, H. F. *Science* **2008**, *321*, 1795–1799.
27. Singh, Y.; Murat, P.; Defrancq, E. *Chem. Soc. Rev.* **2010**, *39*, 2054–2070.
28. Hardman, K. D.; Ainsworth, C. F. *Biochemistry*, **1972**, *11*, 4910–4919.
29. Naismith, J. H.; Field, R. A. *J. Biol. Chem.* **1996**, *271*, 972–976.
30. Mandal D. K.; Kishore N.; Brewer, C. F. *Biochemistry* **1994**, *33*, 1149–1156.

31. Mandal D. K.; Bhattacharyya L.; Koenig S. H.; Brown, III, R. D., Oscarson, S.; Brewer, C. F. *Biochemistry* **1994**, *33*, 1157–1162.
32. Ng, K. K.-S.; Kolatkar, A. R.; Park-Snyder, S.; Feinberg, H.; Clark, D. A.; Drickamer, K.; Weis, W. I. *J. Biol. Chem.* **2002**, *277*, 16088–16095.
33. Sauter, N. K.; Hanson, J. E.; Glick, G. D; Brown, J. H.; Crowther, R. L.; Park, S.-J.; Skehel, J. J.; Wiley, D. C. *Biochemistry* **1992**, *31*, 9609–9621.
34. Leontis, N. B.; Kwok, W.; Newman, J. S. *Nucleic Acids Res.* **1991**, *19*, 759–766.
35. Zhong, M.; Rashes, M. S.; Leontis, N. B.; Kallenbach, N. R. *Biochemistry* **1994**, *33*, 3660–3667.
36. Kadrmas, J. L.; Ravin, A. J.; Leontis, N. B. *Nucleic Acids Res.* **1995**, *23*, 2212–2222.
37. Matsui, M.; Nishiyama, Y.; Ueji, S.; Ebara, Y. *Bioorg. Med. Chem. Lett.* **2007**, *17*, 456–460.
38. Sweeney, E. C.; Tonevitsky, A. G.; Temiakov, D. E.; Agapov, I. I.; Saward, S.; Palmer, R. A. *Proteins: Struct. Func. Genet.* **1997**, *28*, 586–589.

**Figure 1.** Comparison between a structural model for carbohydrate-modified 3-way junction DNAs (A) and 3-dimentional structure of concanavalin A (PDB:1QDC) (B). White arrows indicate the positions of carbohydrate binding sites.

**Figure 2**. Analysis of 3-way junction DNAs. (A) Structure of stems with varying number of unpaired bases in the junction region. The sequences of Strand I, II, and III (18-20 mer) are as follows: 5′-ATCACGCTG-$A_n$-GACTTGCGA-3′ (Strand I), 5′-TCGCAAGTC-$A_n$-TCGCAGGTA-3′ (Strand II), 5′-TACCTGCGA-$A_n$-CAGCGTGAT-3′ (Strand III) (n=0, 1, 2). (B) 20% polyacrylamide gel electrophoresis for Strand I, I+II, and I+II+III. Running conditions: 89 mM Tris-borate, 150 mM NaCl, 5 mM $MgCl_2$, 80 mA, 150 min, 25–28 °C, SYBR Gold staining. (C, D) Profiles of complex ratio ($\alpha$) vs. temperature based on UV melting analyses. The conditions used for UV melting analyses are as follows: [Oligonucleotide]=3 μM, 100 mM $NaH_2PO_4$/$Na_2HPO_4$ (pH 7.0), 150 mM NaCl, with or without 5 mM $MgCl_2$.

**Figure 3**.

Design and analysis of carbohydrate-modified 3-way junction DNAs. (A) Structure of maltose- or lactose-modified deoxyuridine (dU). (B) Structures and sequences of 3-way

junction DNAs (**S3**, **S6**, and **S12**). The distance between the ends of the stems was estimated under the assumptions that the three stems are symmetric and form B-type helices. (C) Sequences of unmodified and maltose-modified double-stranded DNAs (**ds-Native** and **ds-Mal18**). (D) Structure and carbohydrate-modification of each construct. Characters in parenthesis represent modification in Strand I, II, and III: **M**, maltose; **L**, lactose; **0**, unmodified. (E) 12% polyacrylamide gel electrophoresis for unmodified or maltose-modified 3-way junction DNAs. Running conditions: 89 mM Tris-borate, 150 mM NaCl, 5 mM $MgCl_2$, 20 mA, 230 min, 20–25 °C; SYBR Gold staining. 1, Unmodified Strand I (monomer, S6); 2, Unmodified Strand I+II (dimer, S6); 3, Unmodified Strand I+II+III (**S6(0,0,0)**); 4, Maltose-modified Strand I + Unmodified Strand II+III (**S6(M,0,0)**); 5, Maltose-modified Strand I+II + Unmodified Strand III (**S6(M,M,0)**); 6, Maltose-modified Strand I+II+II (**S6(M,M,M)**); 7, Maltose-modified 3-way junction DNA with double-stranded arms (**ds-S6(M,M,M)**). (E) 10% polyacrylamide gel electrophoresis for unmodified and maltose-modified dsDNAs (**ds-Native** and **ds-Ma18**). Running conditions: 1 × TBE, 20 mA, 45 min, SYBR Gold staining. See also Figures S1, S2, and Table S1.

**Figure 4**.

Fluorescence titration assay. (A) Change of fluorescence spectra of FITC-labeled 3-way junction DNA **S6(M,M,M)** at varying concentrations of Con A (from top to bottom, 0 M; 9.1 × $10^{-8}$ M; 1.8, 2.7, 4.5, 7.1, 9.7 × $10^{-7}$ M; 1.2, 1.7, 2.2, 3.0, 4.2, 5.8, 7.7, 9.7 × $10^{-6}$ M; 1.3, 1.7× $10^{-5}$ M). $\lambda_{ex}$=499 nm, $\lambda_{em\ max}$=521 nm. (B, C) Changes in the fluorescence intensity of the FITC-labeled maltose-modified complexes as a function of the Con A concentration. (D) Changes in the fluorescence intensity of the FITC-labeled lactose-modified complexes as a function of the $RCA_{120}$ concentration. The measurements were performed under the following conditions: [FITC-labeled complex]=33 nM, 10 mM Tris-HCl, 150 mM NaCl, 5 mM $MgCl_2$, 0.1 mM $CaCl_2$, and 0.1 mM $MnCl_2$, pH 7.5, 25°C. For competitive binding experiments, 50 mM methyl-$\alpha$-mannopyranoside was added in the buffer. Error bars indicate s.d. from three independent measurements.

**Figure 1**

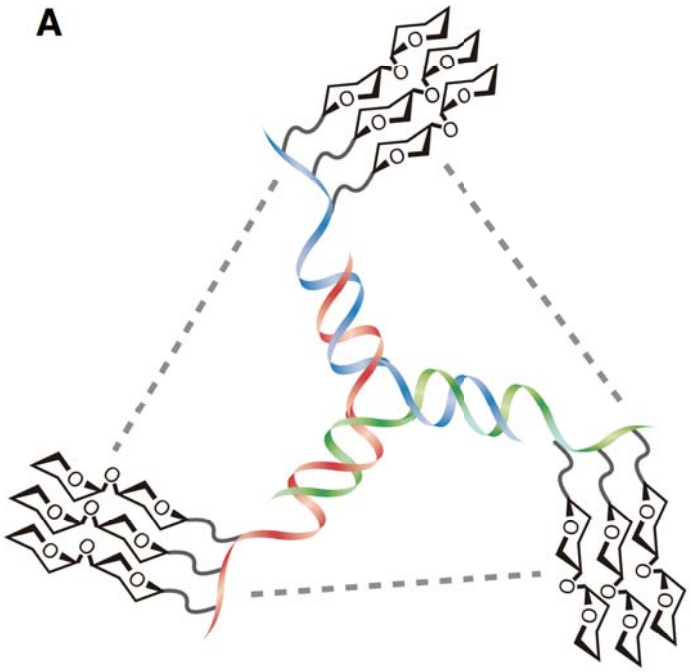


Carbohydrate-Modified 3-Way Junction DNA

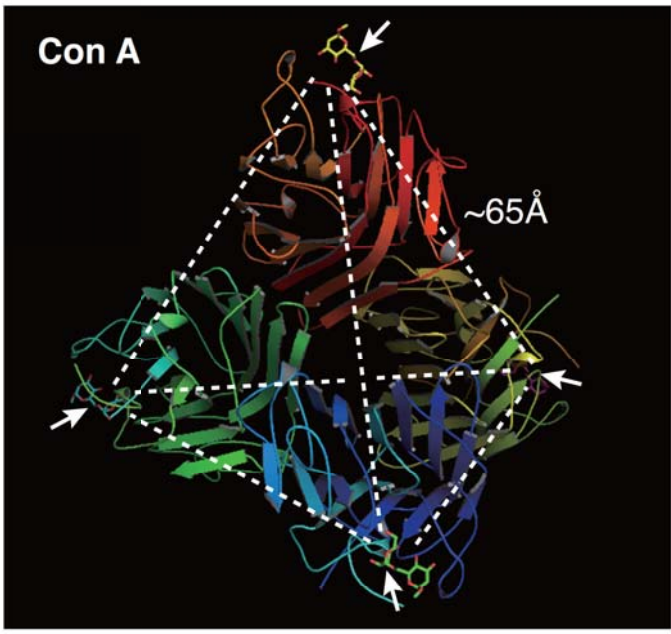

# Figure 2

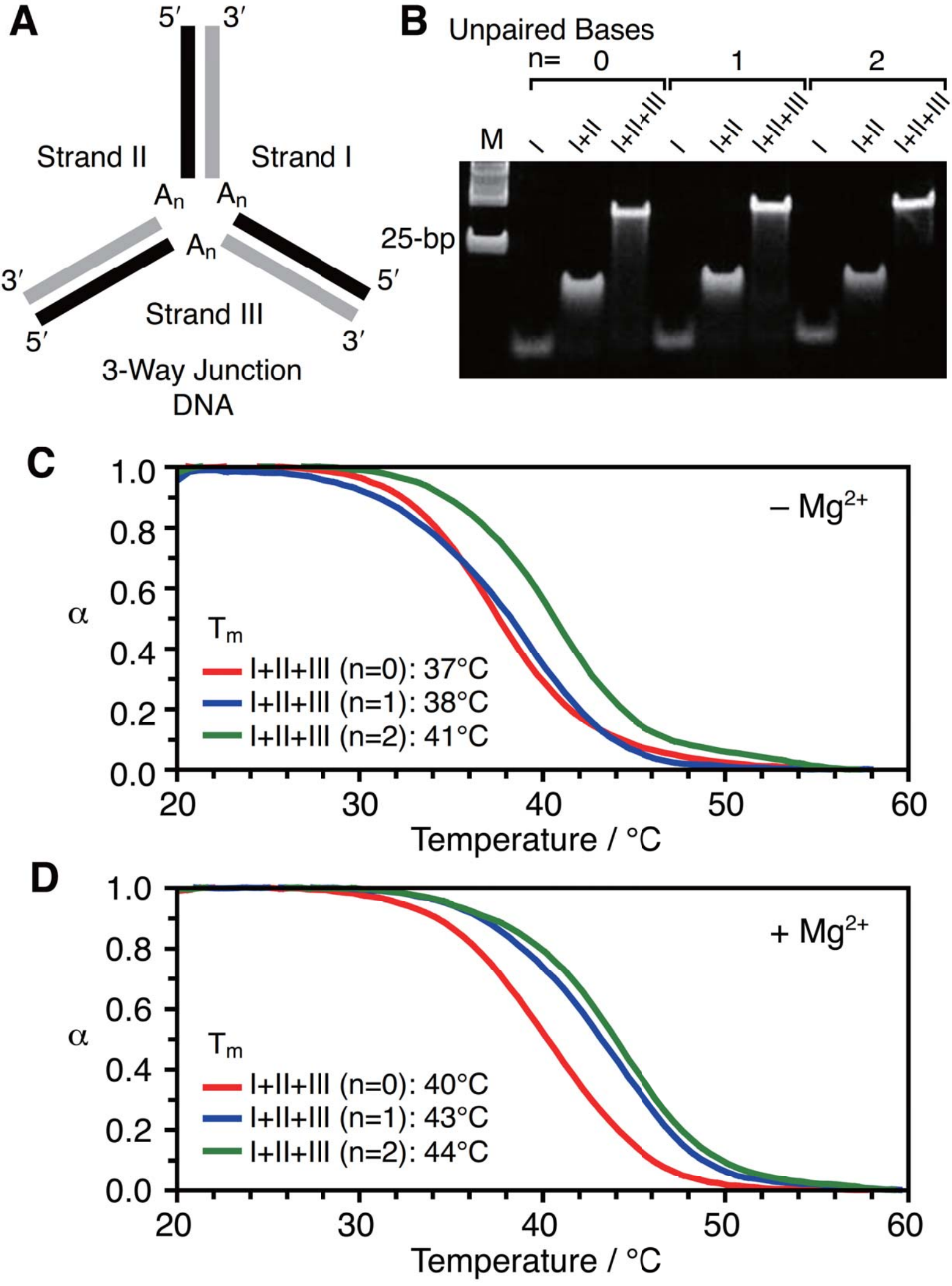
A
5′
3′
Strand II
Strand I
An
An
An
3′
5′
Strand III
5′
3′
3-Way Junction
DNA
B
Unpaired Bases
n= 0
1
2
M
I
I+II
I+II+III
25-bp
C
1.0
0.8
0.6
0.4
0.2
0.0
α
– Mg2+
Tm
I+II+III (n=0): 37°C
I+II+III (n=1): 38°C
I+II+III (n=2): 41°C
20
30
40
50
60
Temperature / °C
D
+ Mg2+
Tm
I+II+III (n=0): 40°C
I+II+III (n=1): 43°C
I+II+III (n=2): 44°C

**Figure 3**

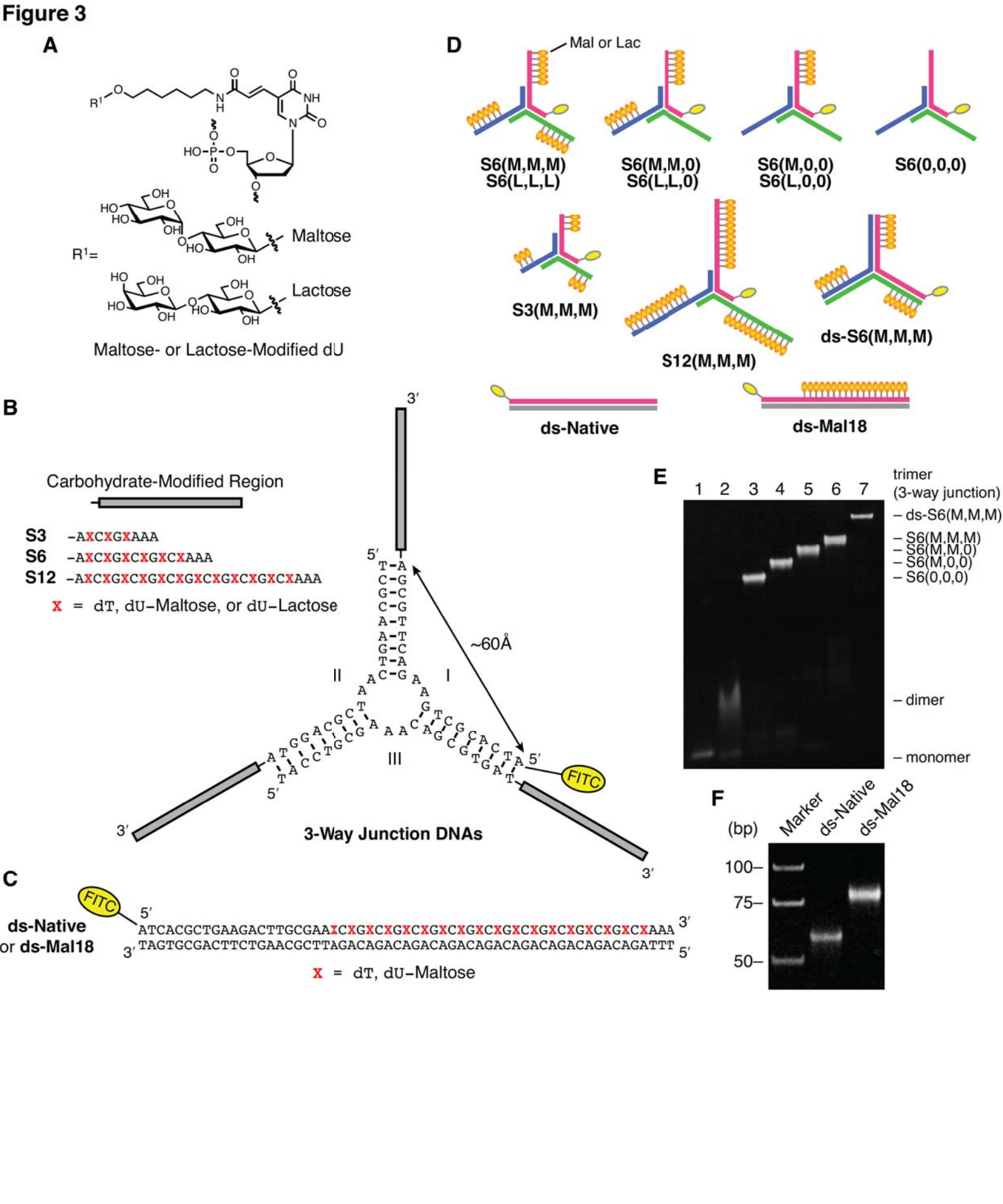
A
R1=
Maltose
Lactose
Maltose- or Lactose-Modified dU
B
Carbohydrate-Modified Region
S3 -AXCXGXAAA
S6 -AXCXGXCXGXCXAAA
S12 -AXCXGXCXGXCXGXCXGXCXGXCXAAA
X = dT, dU–Maltose, or dU–Lactose
3′
5′
~60Å
I
II
III
FITC
3-Way Junction DNAs
C
ds-Native
or ds-Mal18
FITC
5′
ATCACGCTGAAGACTTGCGAAXCXGXCXGXCXGXCXGXCXGXCXGXCXGXCXAAA 3′
3′ TAGTGCGACTTCTGAACGCTTAGACAGACAGACAGACAGACAGACAGACAGACAGATTT 5′
X = dT, dU–Maltose
D
Mal or Lac
S6(M,M,M)
S6(L,L,L)
S6(M,M,0)
S6(L,L,0)
S6(M,0,0)
S6(L,0,0)
S6(0,0,0)
S3(M,M,M)
S12(M,M,M)
ds-S6(M,M,M)
ds-Native
ds-Mal18
E
1 2 3 4 5 6 7
trimer
(3-way junction)
– ds-S6(M,M,M)
– S6(M,M,M)
– S6(M,M,0)
– S6(M,0,0)
– S6(0,0,0)
– dimer
– monomer
F
(bp)
Marker
ds-Native
ds-Mal18
100–
75–
50–

**Figure 4**

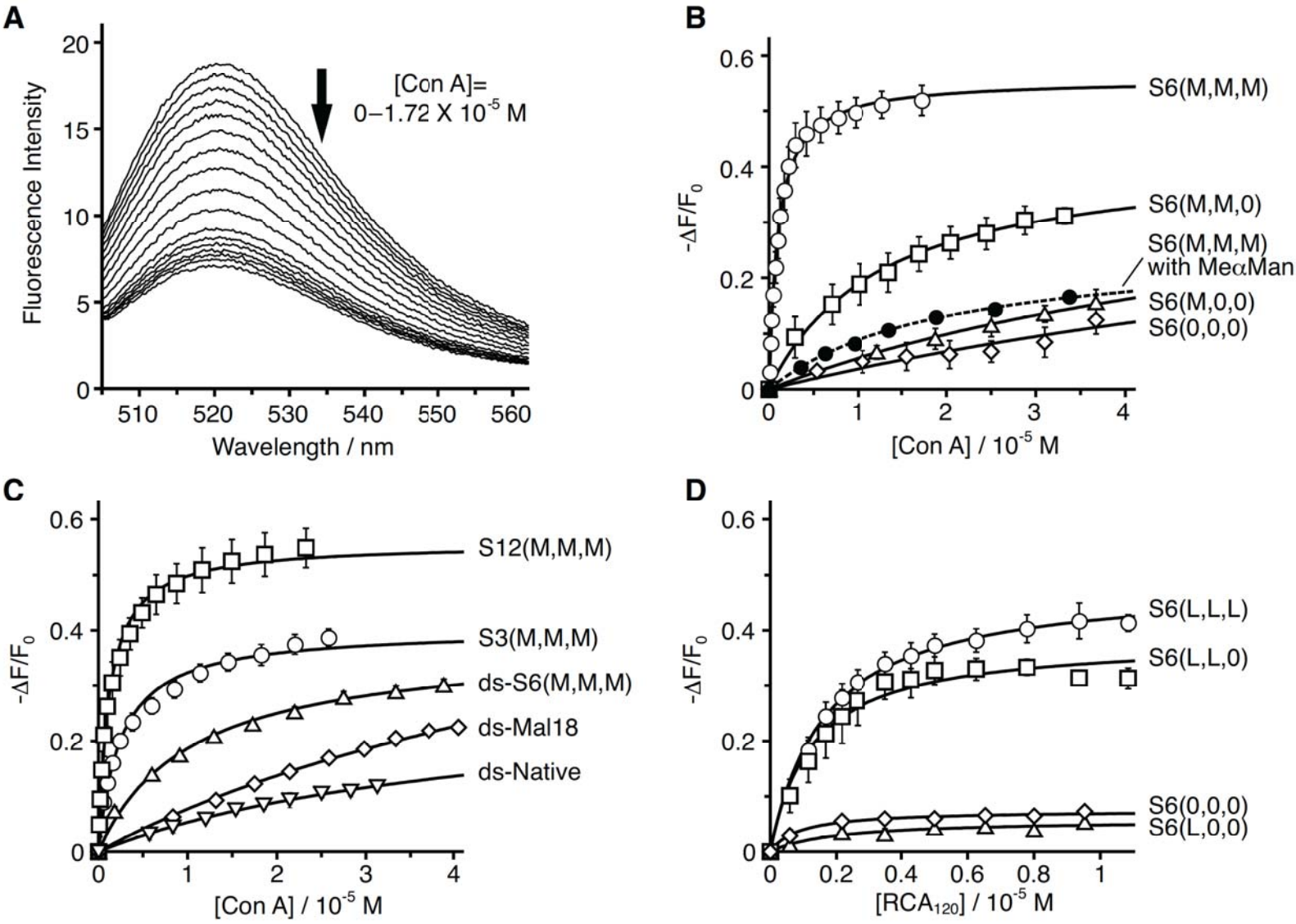
A
Fluorescence Intensity
[Con A]=
0–1.72 X 10-5 M
Wavelength / nm
B
-ΔF/F0
S6(M,M,M)
S6(M,M,0)
S6(M,M,M)
with MeαMan
S6(M,0,0)
S6(0,0,0)
[Con A] / 10-5 M
C
-ΔF/F0
S12(M,M,M)
S3(M,M,M)
ds-S6(M,M,M)
ds-Mal18
ds-Native
[Con A] / 10-5 M
D
-ΔF/F0
S6(L,L,L)
S6(L,L,0)
S6(0,0,0)
S6(L,0,0)
[RCA120] / 10-5 M

**Table 1**. Binding constants ($K_a$) of complexes for Con A or $RCA_{120}$ determined by fluorescence titration assay.

| Target | Complex | Type[a] | Number of Carbohydrates | $K_a$ / $10^6$ $M^{-1}$ |
|---|---|---|---|---|
| Con A | **S6**(M,M,M) | 3WJ | 18 | 1.0 |
| | **S6**(M,M,0) | 3WJ | 12 | 0.084 |
| | **S6**(M,0,0) | 3WJ | 6 | 0.012 |
| | **S6**(0,0,0) | 3WJ | 0 | n.d. |
| | **S3**(M,M,M) | 3WJ | 9 | 0.40 |
| | **S12**(M,M,M) | 3WJ | 36 | 0.79 |
| | **ds-S6**(M,M,M) | 3WJ with double-stranded arms | 18 | 0.10 |
| | **ds-Mal18** | linear double-stranded DNA | 18 | 0.013 |
| | **ds-Native** | linear double-stranded DNA | 0 | n.d. |
| $RCA_{120}$ | **S6**(L,L,L) | 3WJ | 18 | 0.63 |
| | **S6**(L,L,0) | 3WJ | 12 | 1.0 |
| | **S6**(L,0,0) | 3WJ | 6 | n.d. |
| | **S6**(0,0,0) | 3WJ | 0 | n.d. |

[a] 3WJ=3-way junction DNA.

Supplementary Information

# Enhanced Binding of Trigonal DNA-Carbohydrate Conjugates to Lectin

Masayuki Matsui, Yasuhito Ebara

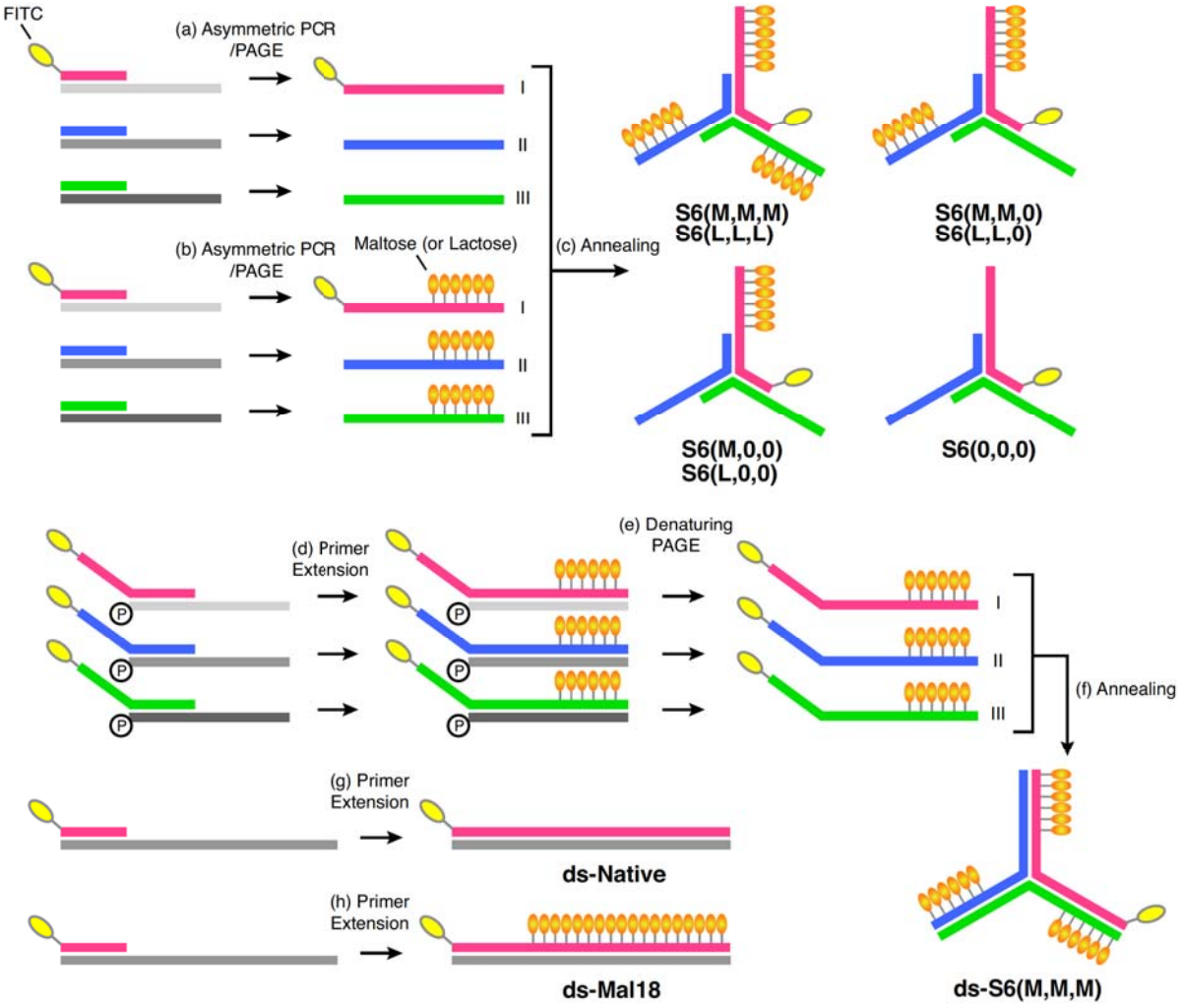


**Figure S1. Schemes and conditions for preparation of 3-way junction DNAs.** (a, b) Asymmetric PCRs and PAGE purification. The reaction mixture contained 0.1 pmol/µl template (S3-I, II, III, S6-I, II, III, S12-I, II, or III), 3 pmol/µl primers (I, II, or III), KOD Dash buffer, 0.2 mM of each dATP+dCTP+dGTP+dTTP (a) or dATP+dCTP+dGTP+dUTP-Mal (b), and KOD Dash DNA polymerase (0.005 U/µl). The thermal cycling profile included an initial denaturation step at 95°C for 5 min, followed by 15–17 cycles of 94°C for 30 sec, 55°C for 30 sec, and 74°C for 1 min. The reaction products were purified by 10% PAGE. Lactose-modified 3-way junction DNAs were prepared in the same way using dUTP-Lac instead of dUTP-Mal. (c, f) Mixture of unmodified or carbohydrate-modified strands I, II, and III was heated at 80°C for 5 min and then gradually cooled for annealing. (d) Primer extension reactions were performed in buffers containing 0.8 pmol/µl templates (S6-I, II, or III phosphorylated at the 3′ ends), 0.8 pmol/µl primer (ext-I, II, or III), 0.2 mM of each dATP+dCTP+dGTP+dUTP-Mal and KOD Dash DNA polymerase (0.005 U/µl) at 50°C for 1 h. (e) 8 M Urea denaturing PAGE. (g, h) Primer extension reactions were performed in buffers containing 0.5 pmol/µl templates (M18), 0.5 pmol/µl primer I, 0.2 mM of each dATP+dCTP+dGTP+dTTP (g) or dATP+dCTP+dGTP+dUTP-Mal (h), and KOD Dash DNA polymerase (0.025 U/µl) at 50°C for 1 h. The products were purified using QIAEX II gel extraction kit.

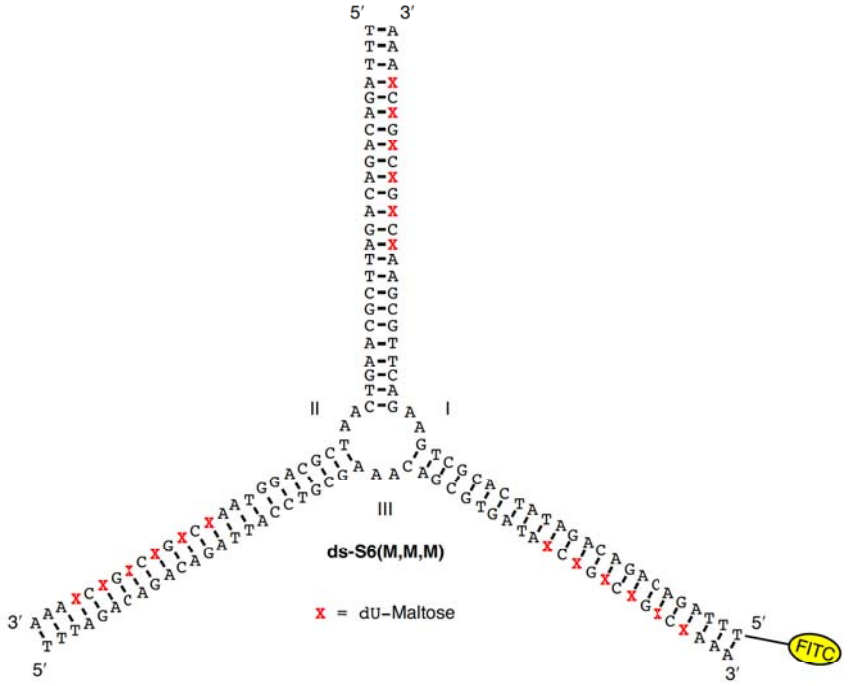


**Figure S2. Design of 3-way junction DNA ds-S6(M,M,M).**

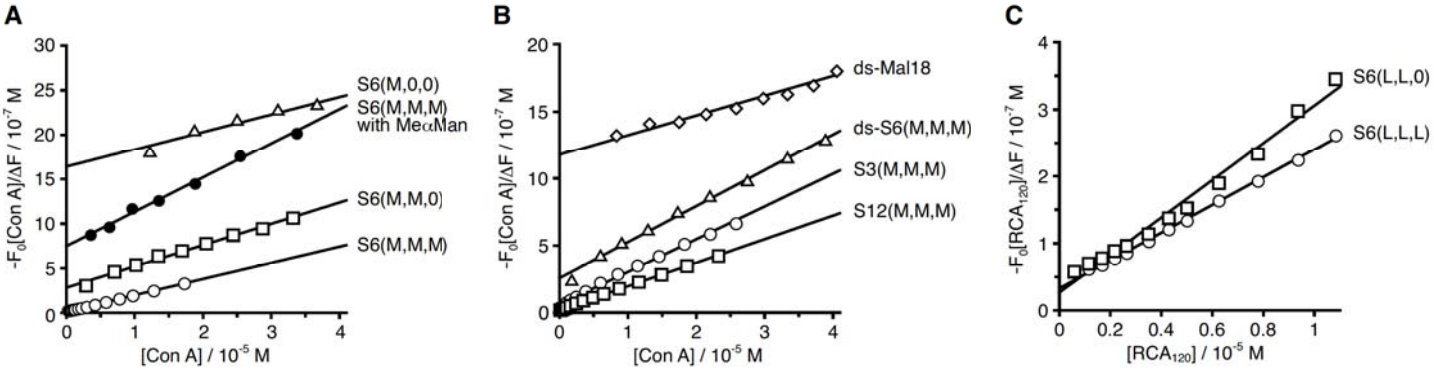


**Figure S3. Determination of binding constants for carbohydrate-modified 3-way junction DNAs or dsDNAs by fluorescence titration assay.** FITC-labeled samples dissolved in the buffer (330 µl) were input into a microcell (1 ml). After varying concentrations of Con A or $RCA_{120}$ solutions were added to the sample and the mixture incubated at 25°C for 10 min, the fluorescence spectra were recorded with excitation at 499 nm. The fluorescence intensity at 521 nm was used to analyze the binding behavior of Con A or $RCA_{120}$ for each construct. The plot of $-F_0$[Lectin]/ΔF vs [Lectin] for each sample was fit to the following equation,

$$\frac{[Lectin]}{-\frac{\Delta F}{F_0}} = \frac{-F_0}{\Delta F_{max}}[Lectin] + \frac{-F_0}{K_a F_{max}}$$

where $F_0$ is the initial fluorescence intensity of the samples corrected for the change in volume, and ΔF is the fluorescence change by adding varying concentrations of lectin solutions (A–C). The binding constants were calculated from the slope and the intercept of the lines.

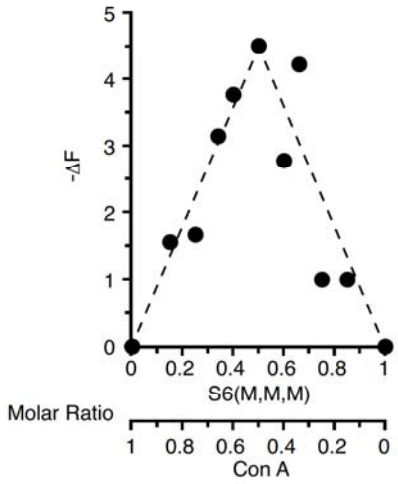


**Figure S4. Job's plot analysis for binding of 3-way junction DNA S6(M,M,M) to Con A.** S6(M,M,M) and Con A were mixed at different molar ratios. The total concentration of S6(M,M,M) and Con A was kept at $2.73X10^{-7}$ M in each sample. The amount of complex formed in each sample was evaluated based on the change of fluorescence at 521 nm.

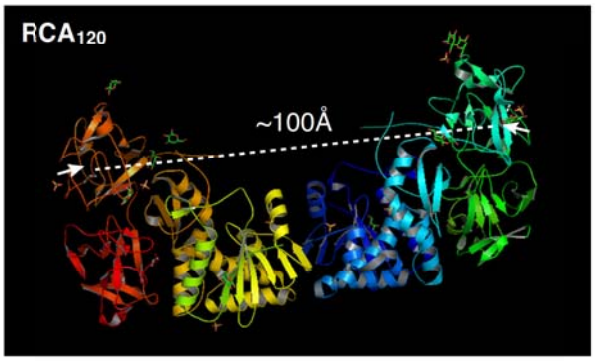


**Figure S5. Binding-site topologies for $RCA_{120}$ (PDB: 1RZO).** White arrows indicate the positions of carbohydrate binding sites.

**Table S1. Sequences of the templates and primers used in this study.**

| | Name | Sequence[a] |
|---|---|---|
| 1 | Template S3-I | TTTACAGATTCGCAAGTCTTCAGCGTGAT |
| 2 | Template S3-II | TTTACAGATTACCTGCGATTGACTTGCGA |
| 3 | Template S3-III | TTTACAGATATCACGCTGTTTCGCAGGTA |
| 4 | Template S6-I[b] | TTTAGACAGACAGATTCGCAAGTCTTCAGCGTGAT |
| 5 | Template S6-II[b] | TTTAGACAGACAGATTACCTGCGATTGACTTGCGA |
| 6 | Template S6-III[b] | TTTAGACAGACAGATATCACGCTGTTTCGCAGGTA |
| 7 | Template S12-I | TTTAGACAGACAGACAGACAGACAGATTCGCAAGTCTTCAGCGTGAT |
| 8 | Template S12-II | TTTAGACAGACAGACAGACAGACAGATTACCTGCGATTGACTTGCGA |
| 9 | Template S12-III | TTTAGACAGACAGACAGACAGACAGATATCACGCTGTTTCGCAGGTA |
| 10 | Template M18 | TTTAGACAGACAGACAGACAGACAGACAGACAGACAGATTCGCAAGTCTTCAGCGTGAT |
| 11 | Primer I | (FITC)-ATCACGCTGAAGACTTGCGA |
| 12 | Primer II | TCGCAAGTCAATCGCAGGTA |
| 13 | Primer III | TACCTGCGAAACAGCGTGAT |
| 14 | Primer ext-I | (FITC)-TTTAGACAGACAGATATCACGCTGAAGACTTGCGA |
| 15 | Primer ext-II | TTTAGACAGACAGATTCGCAAGTCAATCGCAGGTA |
| 16 | Primer ext-III | TTTAGACAGACAGATTACCTGCGAAACAGCGTGAT |

[a] DNA Sequences are listed 5′ to 3′. [b] The template S6-I, II, or III phosphorylated at the 3′ ends was used for the primer extension reaction using the primer ext-I, II, or III.